ELSEVIER

Contents lists available at ScienceDirect

## Journal of Biomechanics

journal homepage: www.elsevier.com/locate/jbiomech www.JBiomech.com



# Fluid-structure interaction modeling of lactating breast: Newtonian vs. non-Newtonian milk



Jamasp Azarnoosh, Fatemeh Hassanipour\*

Department of Mechanical Engineering, The University of Texas at Dallas, 800 W. Campbell Road, Richardson, TX 75080, USA

## ARTICLE INFO

Article history: Accepted 2 May 2021

Keywords: Non-Newtonian fluid Human milk Computational fluid dynamics Fluid-structure interaction

## ABSTRACT

Breastfeeding is a highly dynamic and complex mechanism. The suckling process by the infant involves compression and intra-oral vacuum pressure, leading to milk expression from breast. The accumulated milk from the nipple varies depending on the milk properties and transient flow rate during the suckling cycle. Rheological studies on raw human milk indicate that milk has a non-Newtonian shear-thinning flow behavior. This study aims to investigate the effect of non-Newtonian milk on flow behavior through the breast ductal system using fluid-structure interaction (FSI) simulation. The results of the non-Newtonian effects on flow velocity and the volumetric flow rate of expressed milk are presented. The results show that non-Newtonian Carreau model is promising for the simulation of human milk flow through the breast ductal systems. Also, the results show that the non-Newtonian effects on the milk flow behavior appear for 30–35% of the suckling cycle. Therefore, the Newtonian model is acceptable for the purpose of numerical simulation.

© 2021 Elsevier Ltd. All rights reserved.

## 1. Introduction

The study of breastfeeding mechanism, from an engineering point of view, has attracted the attention of researchers recently (Woolridge, 2019). Computational fluid dynamics (CFD) simulation is a promising tool that has been used recently to explore biotransport milk flow through the ductal system. The numerical simulation studies in the area of breastfeeding assumed milk is a Newtonian fluid (Elad et al., 2014; Mortazavi et al., 2017; Azarnoosh and Hassanipour, 2019b; Azarnoosh and Hassanipour, 2019b; Simulation study by Elad et al. (2014) considered milk with a viscosity of 1 mPa.s. Azarnoosh and Hassanipour (2020) also performed FSI analysis with the Newtonian assumption, by averaging the viscosity from experimental data, which is around 27 mPa.s (Mortazavi et al., 2017).

Experimental studies of the rheology of human milk show it to be a non-Newtonian shear-thinning fluid (pseudoplastic fluid) (Fondaco et al., 2015; Frazier et al., 2016). The most recent study by Alatalo and Hassanipour (2020) further characterized the rheological behavior of human milk by conducting a series of experiments using donated milk.

To the best of the authors' knowledge, there exists no prior numerical simulation in the area of breastfeeding that investigates non-Newtonian flow behavior inside milk ducts. However, several studies exist on blood flow, which is a shear-thinning non-Newtonian fluid, in arteries (Bathe and Kamm, 1999; Johnston et al., 2006), aneurysms (Torii et al., 2009; Morales et al., 2013), aorta, etc. (Liu et al., 2011; Menon et al., 2012). Some studies demonstrate that the assumption of Newtonian fluid for blood flow in large arteries is adequate (Johnston et al., 2004; Johnston et al., 2006; Torii et al., 2006). This observation is dependent on velocity and shear rate in which the apparent viscosity for high shear rate is approximately constant. In contrast, there are studies that emphasize the use of non-Newtonian model in numerical simulations (Gijsen et al., 1999; Chen and Lu, 2006). Despite extensive studies on blood flow, there is no investigation of non-Newtonian milk flow behavior in the breast ductal system.

A recent study by Azarnoosh and Hassanipour (2019a) compared Newtonian and non-Newtonian (power-law model) fluids in a rigid six-generation lobe geometry proposed by Baum et al. (2008). A similar quantitative nature of flow pattern and wall shear stress was observed between the viscous models; however, the power-law non-Newtonian model provides greater milk accumulation compared with the Newtonian flow model. The focus of the present study is to investigate the effects of non-Newtonian milk on flow behavior, such as shear rate, velocity profile, streamlines, and volumetric flow rate (milk removal).

<sup>\*</sup> Corresponding author at: Department of Mechanical Engineering, The University of Texas at Dallas, 800 W. Campbell Road, Richardson, TX 75080-3021, USA. *E-mail address:* fatemeh@utdallas.edu (F. Hassanipour).

A previously developed 3-D computational geometry of lactating breast as well as the pressure data obtained from the clinical data are employed for simulation. Non-Newtonian milk flow is simulated by using power-law, Carreau, Bingham, and Herschel-Bulkley models. The results are discussed for both rigid (without tissue deformation) and deformed structure (elongation of main duct due to vacuum pressure), to quantify the effects of various viscous models.

## 2. Methods

The breast geometry is based on a previous study by Azarnoosh and Hassanipour (2020). An unstructured mesh is generated using ANSYS Meshing tool. The mesh independence study is conducted using the meshes outlined in Table 1.

As detailed in Azarnoosh and Hassanipour (2020), homogeneous incompressible hyperelastic materials were assigned to solid domains. A constant density ( $\rho$ ) of 1026.04 kg/m³ at body temperature was used for the milk sample (Alatalo and Hassanipour, 2020). Four non-Newtonian models outlined in Table 2 are considered for the viscosity ( $\eta$ ) of human milk. The parameters,  $k, n, \lambda, \tau_y, \gamma_c, \eta_0$ , and  $\eta_\infty$  are consistency index, power-law index, time constant, yield stress threshold, critical shear rate, zero shear viscosity, and infinite shear viscosity, respectively. Goodness-of-fit statistics of Root Mean Square Error (RMSE) and R-squared ( $R^2$ ) are provided in Table 2 to quantify the discrepancy between the model and data.

The rheology of various human milk samples showed yield stress when milk starts to flow (Alatalo and Hassanipour, 2020). If the shear stress of fluid is smaller than the yield stress, then the fluid remains rigid. To study this phenomenon, Bingham and Herschel-Bulkley models are considered for analysis. These models are characterized by yield stress, unlike other viscous models in which shear stress is zero at the lowest shear rate.

The experimental data of raw human milk collected by Alatalo and Hassanipour (2020) is used. The viscosity of one milk sample across the shear rate is provided in Fig. 2 as well as Newtonian and non-Newtonian models. Parameters of viscous models are calculated using the Curve Fitting Toolbox in MATLAB. The viscosity of Newtonian fluid is 1.95 mPa.s. Constant viscosity of 1.48 mPa.s (lowest viscosity in data), 1.74 mPa.s (relation between shear stress and shear rate), and 3.74 mPa.s (averaging all viscosity data) are also studied to evaluate the importance of selecting adequate viscosity in numerical simulation.

The non-Newtonian importance factor is considered to evaluate non-Newtonian effects on the milk duct, which is commonly used in study of blood flow. This factor was initially proposed by Ballyk et al. (1994). Johnston et al. (2004) later defined this factor as the ratio of apparent viscosity at any location on surface walls and Newtonian viscosity for infinite shear rate  $(\eta/\eta_{\infty})$ , known as the local non-Newtonian importance factor  $(I_L)$ . When  $I_L$  is close to unity, it represents Newtonian behavior, while a large deviation from unity indicates a non-Newtonian fluid.

The FSI analysis is performed in ANSYS Workbench by coupling flow solver and structural solver as detailed in Azarnoosh and Hassanipour (2020). The governing equations of fluid and solid domains are provided in more detail in Appendix A.

The boundary conditions used for the solid domain follow Azarnoosh and Hassanipour (2020). The nipple deformation was validated with ultrasound images to mimic breastfeeding (Azarnoosh and Hassanipour (2020)). The Newtonian and non-Newtonian fluids outlined in Table 2 are assigned to the fluid domain (lobe). No-slip condition is assumed on the surface wall. The intra-oral vacuum pressure data shown in Fig. 1 is applied at the outlet, which is collected using a tube pressure transducer attached to the breast (Alatalo et al., 2020). The simulation begins with the latch-on (from 0.0 to 2.0 s) and continues with two suckling cycles (from 2.0 to 3.5 s).

Clinical investigations showed that the volume of expressed milk varies from one infant to another depending on the day of feeding. The range of the accumulated milk per cycle for normal breastfeeding varies between 0.1 to 1.3 mL established from Waller et al. (1941), Bowen-Jones et al. (1982), and Mortazavi et al. (2017). This range represents the volume of milk for all active lobes, i.e. 5 to 9 lobes. Averaging this range for a single lobe provides 0.1 mL per cycle. The inlet pressure is adjusted corresponding to the bifurcation number to obtain this volume of milk. The Carreau model is considered as the baseline for comparison with accumulated milk of 0.1 mL/cycle, due to its close fit to experimental data.

#### 3. Results and discussion

To investigate the evolution of milk flow during suckling, the results are presented at the following critical time marks of interest.

- t = 2.02 s, milk starts to flow.
- t = 2.12 s, before transition to Newtonian behavior.
- t = 2.36 s, maximum vacuum pressure.
- t = 2.60 s, after transition to non-Newtonian behavior.
- t = 2.70 s, one step before end of the cycle.

## 3.1. Shear rate and non-Newtonian importance factor

Fig. 3 shows the shear rate and  $I_L$  calculated on the duct surface walls at selected instantaneous times. The results of Carreau model are shown, which is the baseline for comparison. In the rigid body case, milk tends to behave as non-Newtonian fluid before time mark 2.14 s as well as end of the cycle from 2.58 to 2.72 s, showing shear rate less than 50 s<sup>-1</sup>. This indicates that the non-Newtonian effects appear for only 30–35% of the cycle. In the deformed case, the Newtonian behavior can be observed within the main duct and first-generation, which is due to nipple deformation by infant's suckling. The higher generations are farther from infant's suckling and therefore relatively lower shear rate is observed. This shows the noticeable influence of the infant's jaw movement on flow

 Table 1

 Number of nodes and elements of the solid and fluid domains.

Mesh Type	Lobe Models					
	One-generation		Four-generation		Seven-generation	
	Nodes	Elements	Nodes	Elements	Nodes	Elements
Solid (Coarse)	60 k	317 k	221 k	1,213 k	964 k	5,386 k
Solid (Fine)	152 k	801 k	275 k	1,499 k	1,263 k	7,023 k
Fluid (Coarse)	38 k	202 k	264 k	1,380 k	720 k	3,480 k
Fluid (Fine)	70 k	380 k	370 k	1,969 k	1,035	4,753 k

**Table 2**Non-Newtonian viscosity models and calculated parameters.

Model	Equation	Parameters	Accuracy of the model	
Power-law	$\eta=k\gamma^{(n-1)}$	k = 62.84 mPa.s <sup>n</sup> n = 0.034 $\eta_{min}$ =1.48 mPa.s $\eta_{max}$ =61.17 mPa.s	RMSE = $10.90 \times 10^{-4}$ R <sup>2</sup> =97.85%	
Carreau	$\eta = \eta_{\infty} + (\eta_0 - \eta_{\infty}) [1 + (\lambda \dot{\gamma})^2]^{(n-1)/2}$	$\lambda$ =0.579 s n=-0.803 $\eta_0$ =79.03 mPa.s $\eta_\infty$ =1.75 mPa.s	RMSE = $3.31 \times 10^{-4}$ R <sup>2</sup> =99.81%	
Bingham	$\eta = \begin{cases} \frac{\tau_y}{\dot{\gamma}} + k, & \dot{\gamma} \geqslant \dot{\gamma_c} \\ \frac{\tau_y(2 - \dot{\gamma})\dot{\gamma_c}}{\dot{\gamma_c}} + k, & \dot{\gamma} \leqslant \dot{\gamma_c} \end{cases}$	$k = 0.511 \text{ mPa.s}^n$ $\tau_y = 62.41 \text{ mPa}$ $\gamma_c = 1 \text{ 1/s}$	RMSE = $10.12 \times 10^{-4}$ R <sup>2</sup> =98.15%	
Herschel-Bulkley	$\eta = \begin{cases} \frac{\tau_{y}}{\dot{\gamma}} + k(\frac{\dot{\gamma}}{\dot{\gamma}_{c}})^{(n-1)}, & \dot{\gamma} \geqslant \dot{\gamma}_{c} \\ \frac{\tau_{y}(2 - \dot{\gamma})\dot{\gamma}_{c}}{\dot{\gamma}_{c}} + k[(2 - n) + (n - 1)\frac{\dot{\gamma}}{\dot{\gamma}_{c}}], & \dot{\gamma} \leqslant \dot{\gamma}_{c} \end{cases}$	$k = 1.131 \text{ mPa.s}^n$ n = 0.85 $\tau_y = 61.99 \text{ mPa}$ $\dot{\gamma}_c = 0.1567 \text{ 1/s}$	RMSE = $10.43 \times 10^{-4}$ R <sup>2</sup> =98.02%	

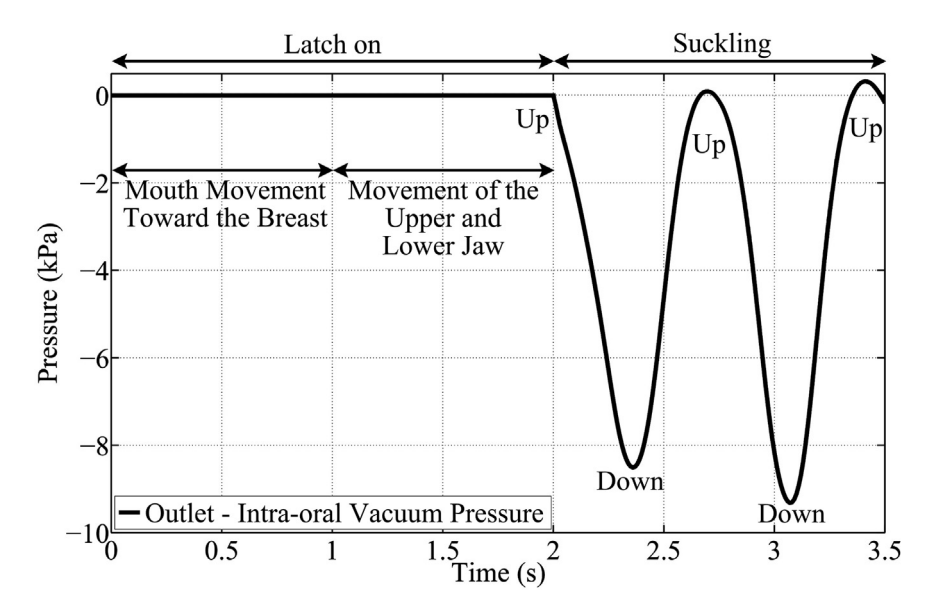
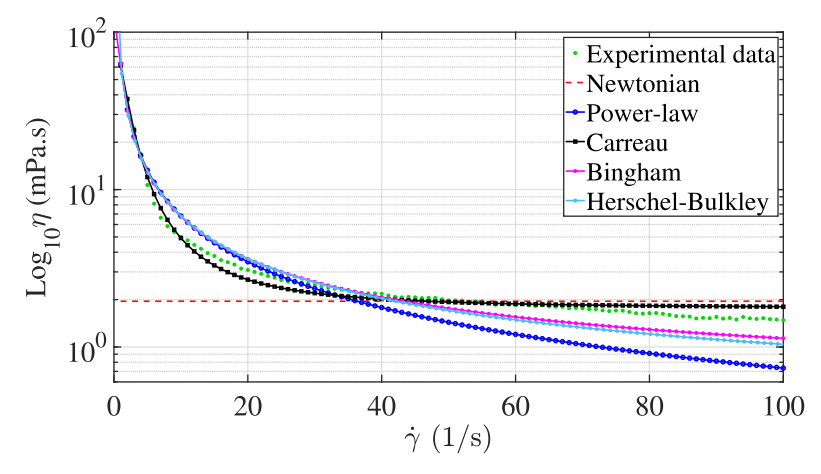


Fig. 1. Intra-oral vacuum pressure profile. The boundary conditions applied to the infant's mouth is shown in various stages. The breastfeeding process starts with the latch on (0.0 to 2.0 s) and follows with two suckling cycles (2.0 to 3.5 s). Adapted from Azarnoosh and Hassanipour (2020).



**Fig. 2.** Viscosity  $(\eta)$  versus the shear rate  $(\dot{\gamma})$  of experimental data (Alatalo and Hassanipour, 2020), Newtonian, and non-Newtonian models.

behavior within the main duct that makes milk behave as a Newtonian fluid. The non-Newtonian behavior with a high value of  $I_L$  is significant in higher generations due to the decrease in the size of

milk ducts. There is no prior study in the area of breastfeeding to compare with the current results; however, this observation is consistent with studies in arteries in which the non-Newtonian

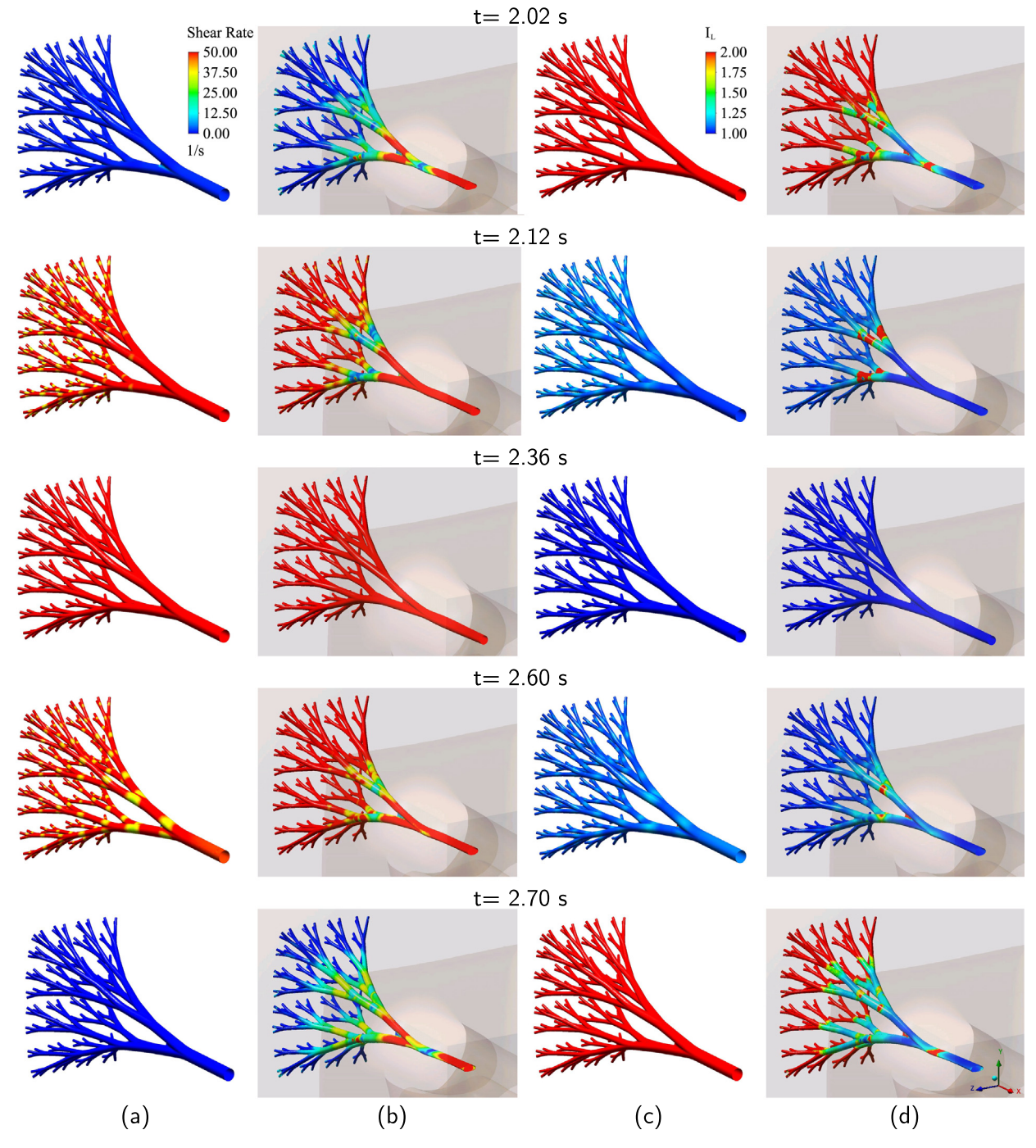


**Fig. 3.** Shear rate and local non-Newtonian importance factor ( $I_L$ ) at five instantaneous times for (a) and (c) rigid body, and (b) and (d) deformed case, respectively.  $I_L$  is calculated using viscosity at any location on surface walls divided by viscosity for infinite shear rate of 1.75 mPa.s in Carreau model. Actual range of shear rate and  $I_L$  varies depending on the time step and viscous model. For Carreau model shown in this figure, the range of global shear rate and  $I_L$  is from 0 to 2024 s<sup>-1</sup> and 1 to 44, respectively.

effects of blood are dependent on the size of artery and flow rate (Johnston et al., 2006; Janela et al., 2010).

## 3.2. Milk flow behavior

The streamline and velocity profiles at the inlet (seventh-generation) and outlet (zeroth-generation) of milk duct for the rigid and FSI simulations at five time marks are provided in Fig. 4. The difference in velocity profile is prominent between Newtonian and non-Newtonian models at the beginning and the end of the cycle. At the lowest vacuum pressure, Newtonian fluid shows a

significantly higher velocity magnitude than other non-Newtonian cases at the inlet and outlet for the rigid body case (see Fig. 4 (a)). In contrast, infant suckling causes significant deformation in the shape of milk duct that leads to variation in milk flow characteristics compared with the rigid body case. This makes non-Newtonian models behave similarly to the Newtonian fluid. This observation implies that vacuum pressure is not the only factor that impacts non-Newtonian behavior of milk flow during suckling. The same phenomenon occurs at end of the cycle.

At 2.14 s, the plug flow region in velocity profile appears in all non-Newtonian cases while the Newtonian case shows a parabolic

## FSI simulation: Newtonian vs. non-Newtonian milk

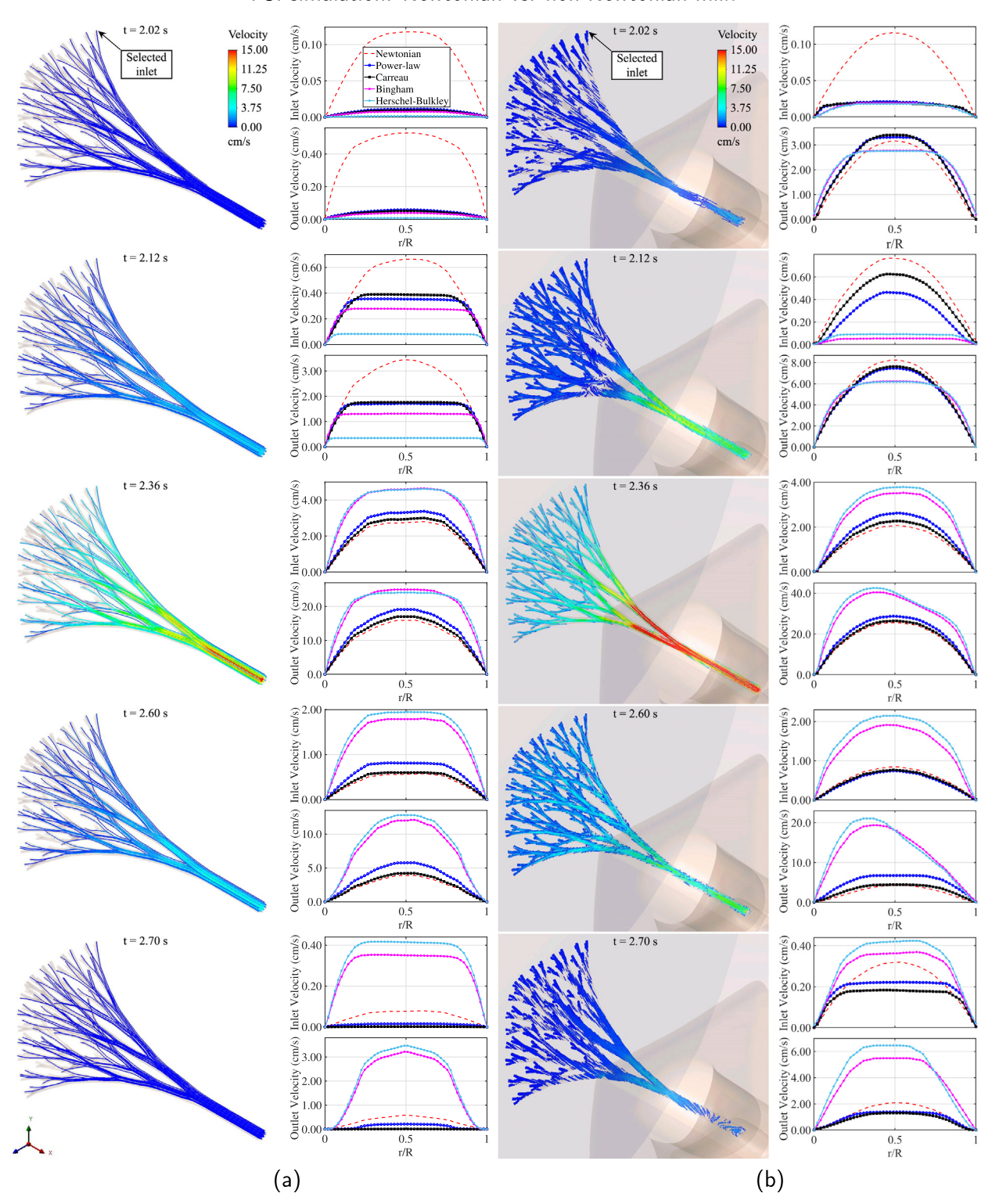


**Fig. 4.** Velocity profile at the inlet and outlet and streamlines, demonstrating overall velocity magnitude through the lobe, at five instantaneous time marks for (a) rigid body and (b) deformed case. In the plots, X-axis represents non-dimensional diameter of the duct. Streamlines shown are the results for Carreau model with the accumulated milk of 0.1 mL per cycle for both rigid body and deformed case. There is a total of 128 inlets for 7-generation lobe model. Velocity profiles are provided for one inlet as specified in the figure.

velocity profile. The influence of jaw movement causes milk to transport in the main duct, leading to a higher velocity gradient compared with the rigid body case, which makes the Newtonian fluid behave very close to the Carreau model. Bingham and

Hershel-Buckley behave differently between the rigid body and the deformed case. This difference is due to the presence of mouthing in the deformed case. The acceleration of velocity in these two models is significant due to the decrease in viscosity at high shear rates.

At peak vacuum pressure (t = 2.36 s), the velocity profile between viscous models is different in magnitude in which the Newtonian case shows the lowest value and Hershel-Buckley the highest. The Newtonian case behaves very similarly to the Carreau model due to its close viscosity to Carreau model. In contrast, the viscosity of Bingham and Hershel-Buckley is smaller, which leads to high velocity gradient. This shows a poor prediction of these two models at high flow rates. As the flow decelerates to transition point (t = 2.58 s), the non-Newtonian models still behave as a Newtonian fluid. The non-Newtonian effects are present from 2.60 s to end of the cycle with the Reynolds number less than 10.

## 3.3. Milk accumulation

The volumetric flow rate and milk accumulation at the outlet are plotted in Fig. 5. Despite the fact that Bingham and Herschel-Bulkley properly predict milk flow at low shear rates, they lead to a greater milk accumulation at high shear rates where viscosity converges to the lowest value (see Fig. 2). This implies that these models are inadequate for simulation of milk hehavior. Similarly, power-law model overestimates milk accumulation compared with the Carreau model. The drawback of using the power-law model is that the results at high flow rates are dependent on the choice of minimum viscosity.

Newtonian model shows fewer accumulated milk compared with the power-law model, which is consistent with previous observations by Azarnoosh and Hassanipour (2019a). The discrepancy between Newtonian and non-Newtonian models appears within the beginning and end of the cycle, showing a poor prediction of Newtonian model. This implies that milk shows non-Newtonian behavior at low shear rates. Despite these differences, the volume of expressed milk for the Newtonian case is 4–8% less

than the Carreau model, which is consistent in both rigid body and deformed case.

Table 3 summarizes the volume of milk per cycle for one-, four-, and seven-generation lobe geometries for viscous models. The Newtonian case shows less milk volume compared with other non-Newtonian models, which is mainly due to the choice of viscosity. Using viscosity of 1.48 mPa.s and 1.74 mPa.s leads to 20–25% and 6–10% greater milk accumulation than Carreau model, respectively. In contrast, viscosity of 3.74 mPa.s from averaging data provides 47–50% less milk. Despite the fact that Newtonian model is acceptable for numerical simulation, choice of the right viscosity value is challenging. At low flow rates, non-Newtonian behavior is significant and choice of average viscosity or minimum viscosity from experimental data may underestimate/overestimate milk accumulation.

A consistent milk accumulation can be seen for Newtonian model as generation level increases in both rigid body and deformed case. In contrast, non-Newtonian models show an increase in accumulated milk for higher generation levels. This indicates that the non-Newtonian effects are prominent through higher generation levels, particularly within the small duct size.

## 4. Conclusion

The objective of this study was to investigate various milk viscosity models in order to perform a reliable CFD simulation of milk flow during breastfeeding. The boundary conditions from clinical data (the vacuum pressure and nipple deformation) were used for the fluid–structure interaction (FSI) simulation presented herein. The numerical simulations were performed assuming a rigid body case and deformed case (FSI analysis) to understand the factors that contribute to milk expression during breastfeeding. Various viscous models were employed for analysis to quantify the difference in milk flow behavior within the milk duct. This study is

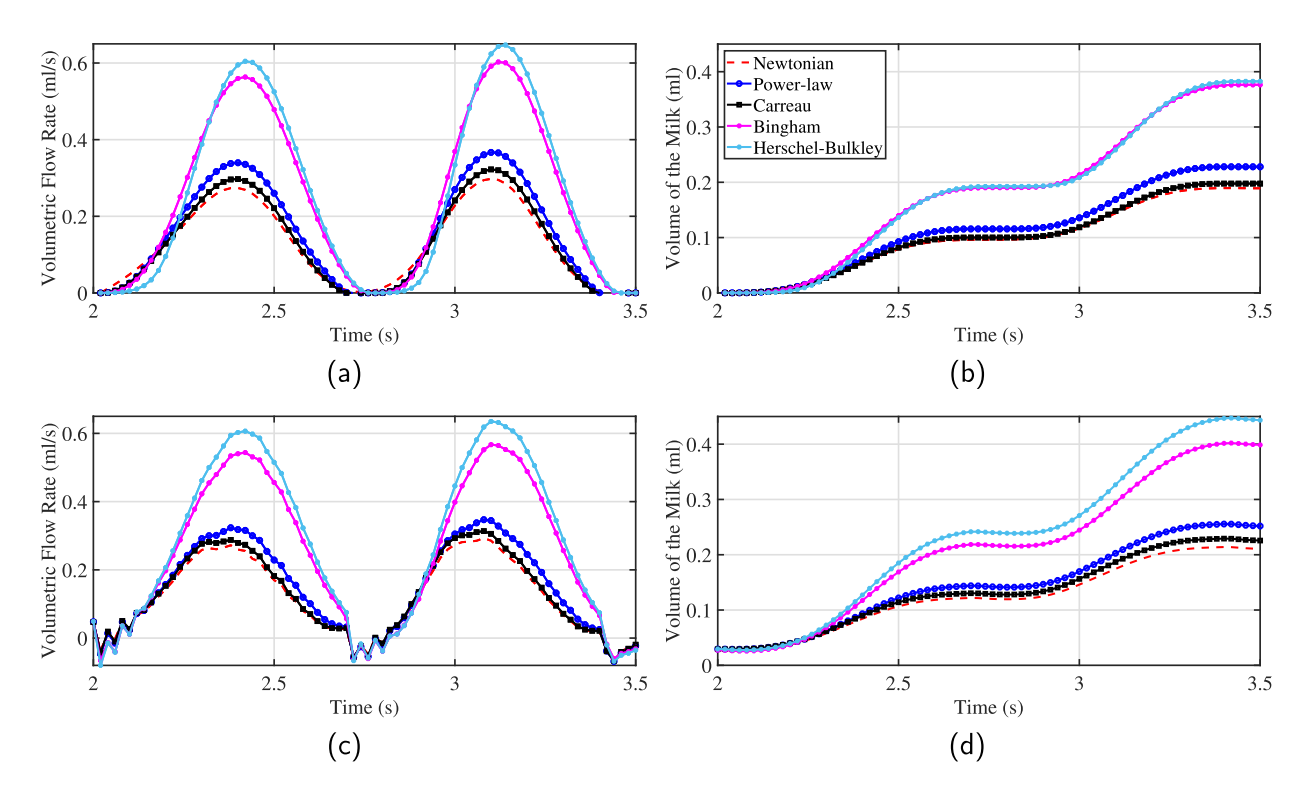


Fig. 5. The volumetric flow rate and volume of the expressed milk for (a) and (b) rigid body, and (c) and (d) deformed case at the outlet, respectively. Newtonian and non-Newtonian cases are plotted within two suckling cycles from 2.0 to 3.5 s.

**Table 3**Comparison of the volume of milk accumulation for different viscous models. The Carreau model is considered as the baseline for comparison with expressed milk of 0.1 mL per cycle.

Viscous model			Rigid body case			Deformed case (FSI)		
	Generation #	One	Four	Seven	One	Four	Seven	
Newtonian	Volume (ml)	0.0958	0.0959	0.0959	0.0920	0.0921	0.0923	
	Error %	4.19	4.08	4.04	7.90	7.81	7.60	
Power-law	Volume (ml)	0.1121	0.1144	0.1155	0.1129	0.1141	0.1154	
	Error %	12.11	14.43	15.55	12.94	14.15	15.47	
Bingham	Volume (ml)	0.1608	0.1796	0.1899	0.1842	0.1929	0.1951	
	Error %	60.88	79.67	89.97	84.21	92.97	95.15	
Herschel-Bulkley	Volume (ml)	0.1661	0.1797	0.1922	0.2068	0.2145	0.2215	
	Error %	66.09	79.79	92.27	106.84	114.50	121.54	
Carreau	Volume (ml)	0.1	0.1	0.1	0.1	0.1	0.1	

novel; it is the first of its kind to numerically investigate the non-Newtonian effects of raw human milk flow during breastfeeding.

The results indicate that milk behaves as a non-Newtonian fluid at low shear rates and Newtonian at high shear rates. The deformation of the ducts during suckling causes milk to behave as a Newtonian fluid within the main duct. Observations have shown that milk flow behavior varies from one location to another and is highly dependent on the shape of the duct subject to deformation. Based on the boundary conditions applied to obtain 0.1 mL per cycle of milk accumulation for the Carreau model, non-Newtonian effects are present during 30–35% of the suckling cycle for the Reynolds number less than 10.

The Bingham and Hershel-Buckley non-Newtonian models were observed to be inadequate because the viscosity for these models at high flow rates converges to the lowest value smaller than the viscosity of experimental data of the milk sample. Hence, the volumetric flow rates and accumulated milk are greater in these two models. The drawback of the power-law model is the choice of the upper and lower bound of the viscosity in which different values of viscosity impact the results of milk accumulation. The non-Newtonian Carreau model is recommended for the numerical simulation of breastfeeding due to its promising behavior at low and high flow rates. Newtonian fluid assumption is acceptable for numerical simulation, but proper caution is required in the choice of the viscosity parameter in the Newtonian model.

The numerical simulations in this study do not capture the entire, complex breastfeeding mechanism; it is limited to a simplified geometry of the mammary ductal system with a single lobe in the human breast. Another limitation is the number of generations (maximum of seven generations) considered for the lobe model. Increasing the generation levels may possibly influence the non-Newtonian behavior during suckling. Incorporating the geometry of a real ductal system for numerical simulation with multiple active lobes may lead to new insights. The analyses were performed using one milk sample. Further investigation is required to quantify non-Newtonian effects using various raw human milk samples.

## **Declaration of Competing Interest**

The authors have no conflict of interest concerning the present manuscript.

## Acknowledgement

This material is based on work supported by the National Science Foundation Grants #1454334, #1614350, and #1707063.

## **Appendix A. Governing equations**

One-way FSI analysis is performed using the partitioned approach by coupling the flow solver (ANSYS Fluent) and a structural solver (ANSYS Mechanical). The physical systems are decomposed into partitions and the solution is obtained separately in each solver.

The fluid is laminar flow due to the low Reynolds number. The governing equations of the fluid domain are based on continuity and Navier–Stokes equations for an isotropic and incompressible fluid flow using the pressure-based scheme (SIMPLE). The discretization approach is finite volume to solve the fluid governing equations as defined in Eqs. A.1 and A.2.

$$\frac{\partial u_i}{\partial x_i} = 0 \tag{A.1}$$

$$\rho \frac{\partial u_i}{\partial t} + \rho \frac{\partial (u_i u_j)}{\partial x_j} = -\frac{\partial p}{\partial x_i} + \frac{\partial \tau_{ij}}{\partial x_j} \tag{A.2}$$

where  $\rho$  is density, u is flow velocity, t is time, p is pressure, and  $\tau_{ij}$  (i, j = 1, 2, 3) is the deviatoric stress tensor, which is relevant to deviatoric strain rate tensor as:

$$\tau_{ij} = 2\eta \dot{\epsilon}_{ij} \tag{A.3}$$

The deviatoric stress tensor  $(\dot{\epsilon}_{ij})$  defined as:

$$\dot{\epsilon}_{ij} = \frac{1}{2} \left( \frac{\partial u_i}{\partial x_i} + \frac{\partial u_j}{\partial x_i} \right) \tag{A.4}$$

For a non-Newtonian fluid, the coefficient  $\eta$  in Eq. A.3 has a non-linear relation between the stress  $(\tau_{ij})$  and strain rate  $(\dot{\epsilon}_{ij})$  depending on shear rate  $(\dot{\gamma})$ , whereas this relation is linear in the Newtonian fluid with a constant viscosity. The non-Newtonian viscosity is only a function of shear rate (i.e.  $\eta_{(\dot{\gamma})}$ ), which is the second invariant of the rate of strain tensor in Eq. A.4 and defined as:

$$\dot{\gamma} = \sqrt{2\sum_{i=1}^{3} \sum_{j=1}^{3} \dot{\epsilon}_{ij} \dot{\epsilon}_{ij}} \tag{A.5}$$

The transient analysis is performed for the solid domain to determine the dynamic response of the structure under time-dependent loads. The governing equation of the solid domain is based on the equation of motion as:

$$[M]\{\ddot{\boldsymbol{U}}_{(t)}\} + [C]\{\dot{\boldsymbol{U}}_{(t)}\} + [K]\{\boldsymbol{U}_{(t)}\} = \{\boldsymbol{F}_{(t)}\}$$
(A.6)

where M, C, and K are the structural mass, damping, and stiffness matrices, respectively. The vectors  $\mathbf{U}_{(t)}$  and  $\mathbf{F}_{(t)}$  are the nodal displacement and applied forces, respectively. The Newmark time integration method is used, which is implicit transient analysis. The analysis is based on finite elements using the Lagrangian formulation.

## References

- Alatalo, D., Hassanipour, F., 2020. An experimental study on human milk rheology: Behavior changes from external factors. Fluids 5, 42.
- Alatalo, D., Jiang, L., Geddes, D., Hassanipour, F., 2020. Nipple deformation and peripheral pressure on the areola during breastfeeding, J. Biomech. Eng. 142.
- Azarnoosh, J., Hassanipour, F., 2019a. Effects of the non-newtonian viscosity of milk flow in the breast ductal system. In: ASME International Mechanical Engineering Congress and Exposition. American Society of Mechanical Engineers, p. V003T04A033.
- Azarnoosh, J., Hassanipour, F., 2019b. Fluid-structure interaction simulation of lactating human breast. In: ASME-JSME-KSME 2019 8th Joint Fluids Engineering Conference. American Society of Mechanical Engineers Digital Collection.
- Azarnoosh, J., Hassanipour, F., 2020. Fluid-structure interaction modeling of lactating breast. J. Biomech., 109640
- Ballyk, P., Steinman, D., Ethier, C., 1994. Simulation of non-newtonian blood flow in an end-to-side anastomosis. Biorheology 31, 565–586.
   Bathe, M., Kamm, R., 1999. A fluid-structure interaction finite element analysis of
- Bathe, M., Kamm, R., 1999. A fluid-structure interaction finite element analysis of pulsatile blood flow through a compliant stenotic artery.
- Baum, K.G., McNamara, K., Helguera, M., 2008. Design of a multiple component geometric breast phantom. In: Medical Imaging 2008: Physics of Medical Imaging. International Society for Optics and Photonics, p. 69134H.
- Bowen-Jones, A., Thompson, C., Drewett, R., 1982. Milk flow and sucking rates during breast-feeding. Develop. Med. Child Neurol. 24, 626–633.
- Chen, J., Lu, X.Y., 2006. Numerical investigation of the non-newtonian pulsatile blood flow in a bifurcation model with a non-planar branch. J. Biomech. 39, 818–832.
- Elad, D., Kozlovsky, P., Blum, O., Laine, A.F., Po, M.J., Botzer, E., Dollberg, S., Zelicovich, M., Sira, L.B., 2014. Biomechanics of milk extraction during breast-feeding. Proc. Nat. Acad. Sci. 111, 5230–5235.
- feeding. Proc. Nat. Acad. Sci. 111, 5230–5235.
  Fondaco, D., AlHasawi, F., Lan, Y., Ben-Elazar, S., Connolly, K., Rogers, M., 2015.
  Biophysical aspects of lipid digestion in human breast milk and similac infant formulas. Food Biophys. 10, 282–291.
- Frazier, J., Chestnut, A.H., Jackson, A., Barbon, C.E., Steele, C.M., Pickler, L., 2016. Understanding the viscosity of liquids used in infant dysphagia management. Dysphagia 31, 672–679.

- Gijsen, F.J., van de Vosse, F.N., Janssen, J., 1999. The influence of the non-newtonian properties of blood on the flow in large arteries: steady flow in a carotid bifurcation model. J. Biomech. 32, 601–608.
- Janela, J., Moura, A., Sequeira, A., 2010. A 3d non-newtonian fluid-structure interaction model for blood flow in arteries. J. Comput. Appl. Math. 234, 2783–2791
- Johnston, B.M., Johnston, P.R., Corney, S., Kilpatrick, D., 2004. Non-newtonian blood flow in human right coronary arteries: steady state simulations. J. Biomech. 37, 709–770
- Johnston, B.M., Johnston, P.R., Corney, S., Kilpatrick, D., 2006. Non-newtonian blood flow in human right coronary arteries: transient simulations. J. Biomech. 39, 1116–1128.
- Liu, X., Fan, Y., Deng, X., Zhan, F., 2011. Effect of non-newtonian and pulsatile blood flow on mass transport in the human aorta. J. Biomech. 44, 1123–1131.
- Menon, A., Wendell, D.C., Wang, H., Eddinger, T.J., Toth, J.M., Dholakia, R.J., Larsen, P. M., Jensen, E.S., LaDisa Jr, J.F., 2012. A coupled experimental and computational approach to quantify deleterious hemodynamics, vascular alterations, and mechanisms of long-term morbidity in response to aortic coarctation. J. Pharmacol. Toxicol. Methods 65, 18–28.
- Morales, H.G., Larrabide, I., Geers, A.J., Aguilar, M.L., Frangi, A.F., 2013. Newtonian and non-newtonian blood flow in coiled cerebral aneurysms. J. Biomech. 46, 2158–2164.
- Mortazavi, S.N., Geddes, D., Hassanipour, F., 2017. Lactation in the human breast from a fluid dynamics point of view. J. Biomech. Eng. 139, 011009.
- Torii, R., Oshima, M., Kobayashi, T., Takagi, K., Tezduyar, T.E., 2006. Fluid-structure interaction modeling of aneurysmal conditions with high and normal blood pressures. Comput. Mech. 38, 482–490.
- Torii, R., Oshima, M., Kobayashi, T., Takagi, K., Tezduyar, T.E., 2009. Fluid-structure interaction modeling of blood flow and cerebral aneurysm: significance of artery and aneurysm shapes. Comput. Methods Appl. Mech. Eng. 198, 3613–3621
- Waller, H., Aschaffenburg, R., Grant, M.W., 1941. The viscosity, protein distribution, andgold number'of the antenatal and postnatal secretions of the human mammary gland. Biochem. J. 35, 272.
- Woolridge, M., 2019. The biomechanics of breastfeeding: bridging the gap between engineering-based studies and clinical practice. Human Milk: Composition, Clinical Benefits and Future Opportunities, vol. 90. Karger Publishers, pp. 13–32.